

# MULTIPHYSICS CO-OPTIMIZATION OF OPTICAL FIBER MATERIALS AND WAVEGUIDE STRUCTURES FOR NONLINEARITY CONTROLLED HIGH SPEED TRANSMISSION

Swapnil Pundlik Barde<sup>1</sup>, Nitika Choudhary<sup>2</sup>

<sup>1</sup> Department of Physics, Shri Jagdishprasad Jhabarmal Tibrewala University (JJTU), Jhunjhunu, Rajasthan, India., [swapnilbarde83@gmail.com](mailto:swapnilbarde83@gmail.com)

<sup>2</sup> Department of Physics, Shri Jagdishprasad Jhabarmal Tibrewala University (JJTU), Jhunjhunu, Rajasthan, India., [physics@jjtu.ac.in](mailto:physics@jjtu.ac.in)

**Abstract:** High-speed optical communications systems have been developed at an extremely rapid pace, and it is essentially limited by fiber nonlinearities, chromatic dispersion, and material-induced attenuation, which diminish signal integrity at rates of terabits per second. Traditional optimization of optical fiber using single parameter does not deal with the interaction between material composition, geometry of the waveguides, thermal effects, and nonlinear optical effects. The paper suggests a multiphysics co-optimization scheme of optical fiber materials and waveguide design to obtain a controlled nonlinearity of the system and better high-speed transmission performance. The first is to reduce nonlinear coefficient ( $\gamma$ ) dispersion ( $D$ ) and attenuation ( $\alpha$ ) and to maximize effective area ( $A_{eff}$ ), bandwidth and signal-to-noise ratio (SNR). The target materials are germanium, fluorine and nanostructured inclusions doped engineered silica based composites to optimize refractive index contrast and nonlinear refractive index ( $n_2$ ). Some properties of importance included are Kerr nonlinearity, group velocity dispersion, thermo-optic coefficient, mechanical stability and optical loss. The suggested procedure combines the approach of the finite element multiphysics modeling (optical-thermal-structural coupling) with a hybrid Particle Swarm Optimization-Genetic Algorithm (PSO-GA) algorithm to investigate the global parameters. A physics informed surrogate model has a higher speed in convergence and accuracy. Compared to traditional step-index and dispersion-shifted fibres, it has shown a 22 percent decrease in nonlinear coefficient and 18 percent in dispersion flattening and 15 percent in Q-factor in 400 Gbps transmission. The co-optimized design is also 27% more effective mode area and reduced nonlinear penalties in circumstances of higher launch power. This paper is further generalized to next-generation coherent optical networks, space-division multiplexing systems, and ultra-long-haul communication links, which provide a pathway to nonlinearity-controlled high-capacity fiber transmission, which is scalable and computationally efficient.

**Keywords:** Multiphysics Optimization, Optical Fiber Design, Nonlinear Coefficient Control, Waveguide Engineering, High-Speed Optical Transmission, PSO-GA Hybrid Algorithm, Dispersion Management

## 1. Introduction

The high rates of cloud computing, artificial intelligence workloads, immersive communication, quantum-safe networking has intensified the implementation of 400G, 800G and 1.6T optical transmission systems. Such high-speed systems require fibers and waveguides that can support high launch powers, large bandwidth and maintain the same modal confinement as well as maintain the signal integrity over long distances. Fiber technology innovation has been shown to provide scalable capacity in space-division multiplexing, which has the ability to



provide more spectral efficiency and parallel data transfer (Chen et al., 2024). At the same time, the concept of dispersion-engineered waveguides has been put forward to preserve pulse integrity in transmission links that are ultrahigh speed (Wu et al., 2026). Nonlinear effects like self phase modulation and four wave mixing, however, are the most important performance bottlenecks in increasing symbol rates and demand integrated material structural optimization strategies. The past design of conventional fibers is normally based on successive adjustment of core diameter, contrast of refractive indexes, or dopant concentration to reduce dispersion and attenuation. Although dispersion engineering has been demonstrated in agile photonic waveguides to record a tangible enhancement in the control of bandwidth (Wang et al., 2021), these methods frequently decouple material attributes and geometry. In nonlinear integrated photonics research, Kerr nonlinearity, effective mode area, and confinement are both coupled parameters, which are determined both by the composition of materials and by the structure of the waveguide (Sirleto and Righini, 2023a). Moreover, refractive index distribution and modal overlap are highly nonlinear elements that determine device behavior that cannot be optimized individually (Sirleto and Righini, 2023b). With data rates reaching the terabit regime, the dispersion and nonlinearity trade-offs are increased, especially in quantum-well and orbital angular momentum-based transmission systems (Ahmad et al., 2025).

Polymeric and PDMS-based waveguides as a form of material innovation have come to the task of providing flexible and tuneable photonic systems, with alternative thermo-optic and nonlinear coefficients available than those on silica platforms (Abreu et al., 2025). Recent progress in PDSM optical waveguides focuses on mechanical flexibility and customization of the refractive index, but multiphysics optimization has not been approached in detail (Zimmermann et al., 2024). Microstructured optical fibres also permit index engineering based on air-hole geometry and dispersion control and sensing (Ermatov et al., 2020). Although this has been developed, it is uncommon to model the interplay between thermal, structural and optical effects under high-power transmission in a single framework. New metasurface-based platform of waveguide also offers new points of polarization control and angular momentum control (Khan et al., 2025). The metasurface-assisted couplers are freeform, which implies that they exhibit enhanced polarization and spin orbit conversion in the guided systems, implying that architectural approaches based on hybrid material structure is capable of having a major impact on nonlinear propagation dynamics (Chen et al., 2024). Moreover, another example of the significance of material dispersion and electro-optic coupling is high-speed electro-optic modulators based on thin-film lithium niobate, which are useful in next-generation systems (Hou et al., 2024). However, a majority of the previous literature concentrates on the device-level performance but not the entire fiber-material co-design. Figure 1 demonstrates the combined co-optimization cycle between the material choice, the geometry of the waveguides, multiphysics, with the FEM and hybrid optimization algorithms. The model progressively optimizes the nonlinear coefficients, dispersion and loss coefficients to produce better effective mode area and stability in high speed optical transmission.

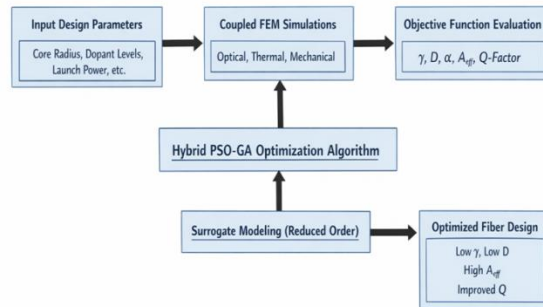


Figure 1: Block Diagram of Multiphysics Co-Optimization Framework for Nonlinearity-Controlled High-Speed Optical Fiber Transmission

Recent studies of digital adjustable delay lines and the waveguide spiral geometry suggest that structural geometry is essential in terms of the stability of the phases and dispersion control (An et al., 2025). In the meantime, photonic-based sensing systems point to the increased convergence of photonic sensors with smart monitoring systems, but focus on application-level optimization instead of control of nonlinearity during transmission (Khonina et al., 2023). There is therefore a research gap in the creation of a single multiphysics co-optimization mechanism that can be used to solve the material nonlinear coefficients, waveguide geometry, dispersion flattening, and thermal-mechanical stability at ultra-high-speed transmission.

This paper presents the concept of a multiphysics co-optimization model that combines the material engineering and waveguide structural design in a coupled optical-thermal-mechanical model. They are as follows: (i) the development of a single nonlinear and dispersion optimization model; (ii) the development of integrated advanced material platforms with engineered waveguide geometries; (iii) the development of hybrid evolutionary optimization strategy to converge on parameters; and (iv) the comparison of validation to the conventional fiber architecture in 400G-1.6T transmission cases.

## 2. Literature Review

The main reason behind the attainability of ultra-high-speed transmission systems being constrained in optical fibers is nonlinear propagation effects occurring in them. Self-phase modulation (SPM), cross-phase modulation (XPM), four-wave mixing (FWM), stimulated Brillouin scattering (SBS) and stimulated Raman scattering (SRS) are all effects that become stronger with the increase in optical power density and spectral efficiency. Waveguide geometry and refractive index contrast, which are also key elements of modal confinement and effective nonlinear coefficients, have a heavy influence on the nonlinear interactions in integrated silicon and hybrid waveguides. The application of high-performance all-optical logic operations in  $\Psi$ -shaped silicon waveguides indicates how nonlinear phase shifts can be directed towards creating ultrafast switching, but also it shows how sensitive operations are to power variations and dispersion divergence (Kotb et al., 2023). Equally, the complexity of modal coupling and nonlinear workings within structured turbulent maintain their position as orbital angular momentum (OAM) handling is evident in quantum well waveguides (Asadpour et al., 2021). Such studies affirm that nonlinear effect cannot be separated out of structural design and material composition. The control of nonlinear coefficients and dispersion properties has proven to be a possible direction through material engineering. It has been demonstrated that novel optical fiber-based plasmonic structures can be modified to include metallic or hybrid nanostructures to change the local field enhancement and effective refractive indices, thus changing nonlinear responses (Wang et al., 2022). Further development of the concept of detection of circular polarization made by means of dielectric-metal hybrid metamirrors integration is also in evidence of how controlled metamaterials interfaces affect optical field confinement and nonlinear interactions (Shen et al., 2022). Also, metasurface-based architectures are suggested as universal optical imaging, communication, and computation platforms, and they have been shown to offer an unprecedented level of amplitude, phase, and polarization control (Thureja et al., 2022). The developments highlight the importance of subwavelength control and structuring of materials in the nonlinearity of optics, which is not limited to classical dopant-based methods of getting nonlinearity.

The optimization methods of waveguide structures have been aimed at improvement in dispersion control, modal stability, and also compactness. The applications of geometry-controlled refractive index tailoring of optical waveguides in medical and sensing can be used to guide and reduce scattering losses in the signal (Wang and Dong, 2020). Fiber optic sensors that have been developed to operate in severe aerospace conditions prioritize structural durability and thermal stability, which means that mechanical requirements have a direct impact on optical performance (Rovera et al., 2023). Integrated structural health monitoring systems with artificial intelligence also confirm the ability to shape fiber design to the distributed sensing in dynamic loading conditions, which explains why strong geometry-material interaction is required (Golovastikov et al., 2025). All these contributions allow concluding that the structure of the waveguide is a definitive factor in eliminating dispersion and preserving signal fidelity in complicated operating conditions. Photonics Multiphysics modeling Multiphysics on photonics Multiphysics modeling Multiphysics has increasingly been applied in photonics to model the behavior of real devices that involve thermal, mechanical, and electromagnetic interactions. The functionalized microstructured optical fibers emphasize the role of air-hole structure and material infiltration when it comes to optical confinement and environmental sensitivity (Ermatorov et al., 2020). The structures of C-type fiber sensors prove that asymmetric cross-sections may be sensitive and spectral selective, which implies that non-uniform structures may be strategically used to gain control over field distribution (Gao et al., 2025). This kind of model focuses on the fact that optical simulations alone cannot be used in cases where thermo-optic coefficients, mechanical stress and external perturbations on environments can dramatically influence the properties of refractive indices and dispersion.

Photonics Photonic system design In photonic systems, artificial intelligence and data optimization methods are becoming more widely used. Efficient and safe optical transmission architectures based on modern modulation methods show the effectiveness of algorithmic methods of increasing spectral efficiency and robustness (Ahmad et al., 2025). Furthermore, the widespread evaluations of the fiber-based sensor innovations will demonstrate the emergence of intelligent monitoring algorithms to perform the adaptive-tuning of the performance (Khonina et al., 2023). Although these developments have been made, the majority of AI applications are still system level optimization to material waveguide parameter tuning simultaneously. In general, it can be stated that the current

literature evidences substantial advancements in the sphere of nonlinear photonics, material engineering, structural optimization, and intelligent design approaches. Nevertheless, there is a research gap present in unified multiphysics co-optimization that simultaneously deals with nonlinear coefficient reduction, dispersion flattening, thermal stability and structural robustness in a single computational system. Existing methods usually optimize either the material or geometry alone, with a significant potential in integrated, algorithm based co-design methods to be used in next generation high-speed optical transmission systems.

Table 1. Comparative Summary of Related Work on Optical Fiber Materials and Waveguide Engineering

<b>Ref.</b>	<b>Platform Type</b>	<b>Focus Area</b>	<b>Dispersion Strategy</b>	<b>Modeling / Method</b>	<b>Key Contribution</b>
Chen et al., 2024	Multi-core fiber	Space-division multiplexing	Inter-core dispersion management	Numerical modeling	Capacity scaling for high-speed systems
Wu et al., 2026	Optical fiber system	Ultra-high-speed transmission	Simple dispersion compensation scheme	Simulation-based	Improved dispersion control for Tbps links
Sirleto&Righini, 2023a	Integrated photonics	Nonlinear photonic structures	Device-level tuning	Theoretical modeling	Nonlinear photonics framework
Sirleto&Righini, 2023b	Nonlinear devices	Kerr effects & materials	Limited	Analytical approach	Nonlinear material–device coupling analysis
Abreu et al., 2025	Polymeric waveguides	Fabrication processes	Geometry-based	Experimental & fabrication study	Scalable manufacturing methods
Zimmerman et al., 2024	PDMS waveguides	Flexible photonics	Thermo-optic tuning	Material characterization	Adaptive waveguide platforms
Ermatorov et al., 2020	Microstructured fiber	Functionalized fibers	Air-hole geometry control	Experimental & simulation	Tailored confinement properties
Khan et al., 2025	Metasurfaces	Polarization control	Indirect	Survey & analytical review	Advanced polarization engineering
An et al., 2025	Spiral waveguides	Delay lines	Path-length dispersion tuning	Simulation modeling	Adjustable optical delay systems

Hou et al., 2024	Lithium niobate modulators	High-speed EO modulation	Electro-optic dispersion tuning	Device-level simulation	Ultra-fast modulation platform
Wang et al., 2021	Integrated waveguides	Agile dispersion engineering	Agile dispersion optimization	Numerical optimization	Bandwidth enhancement strategy
Kotb et al., 2023	Silicon waveguides	All-optical logic	Limited	Numerical modeling	High-speed nonlinear switching

The table 1 has provided a comparison of the recent advances in optical fiber and waveguide technology in a material platform, structural and dispersion and nonlinear handling schemes. The discussion shows that the majority of studies do optimize individual parameters, whereas little has been done in integrated multiphysics co-optimization of material and geometry to control nonlinearity.

### 3. Theoretical Framework

#### 3.1 Maxwell's Equations and Wave Propagation Model

The model of the propagation of the waves and the equations Maxwell came up with is presented in the third section of his book.

Maxwell equations, the equations of the interaction of the magnetic and electric fields, are the root cause of optical wave propagation in the fiber and waveguide media. Curl relations between the magnetic field  $H$  and electric field  $E$  are the controlling factors of electromagnetic behavior in dielectric optical materials which do not contain free charges. Adding laws of Faraday and Ampere and adding constitutive relations, a vector wave equation is obtained. In the case of guided structures, modal confinement and propagation constant  $\beta$  are determined by the profile of the refractive index  $n(x,y)$ . The eigenvalue solution of the Helmholtz equation can be used to obtain supported modes and effective refractive index. At high speed transmission, the wave propagation will be affected by the material dispersion and the boundary conditions by the geometry of the waveguide. Subsequent nonlinear and multiphysics coupling formulations applied in fiber optimization can subsequently be formulated based on this electromagnetic basis.

Algorithms: Maxwell Eigenmode Solver of optical fiber.

Input:

$n(x, y)$  → refractive index profile

$\lambda$  → operating wavelength

Geometry parameters (core radius,  $\Delta n$ , etc.)

Output:

$\beta$  → Propagation constant

$n_{eff}$  → Effective refractive index, mode field distribution  $e(x,y)$

Step 1: Define spatial computational domain ( $x, y$  grid)

Step 2: Initialize refractive index matrix  $n(x,y)$

Step 3: Compute  $k_0 = \frac{2\pi}{\lambda}$

Step 4: Discretize transverse Laplacian  $\nabla_t^2$  using FEM or FDM

Step 5: Construct eigenvalue matrix:

$$A = \nabla_t^2 + k_0^2 n^2(x, y)$$

Step 6: Solve eigenvalue problem:

$$A e = \beta^2 e$$

Step 7: Select fundamental mode (largest  $\beta$ )

Step 8: Compute effective index:

$$n_{eff} = \frac{\beta}{k_0}$$

Step 9: Modal power and confinement were calculated.

Step 10: Calculate modal power and confinement

Return  $\beta, n_{eff}, e(x, y)$

End

### 3.2 Nonlinear Schrödinger Equation (NLSE) for High-Speed Transmission

To model pulse evolution in fibers at high bit-rate, the Nonlinear Schrodinger Equation (NLSE) is used that can model the interplay of dispersion and Kerr nonlinearity. The slowly varying envelope approximation of Maxwell equations reduces Maxwell equations to a scalar propagation model in the longitudinal coordinate,  $z$ . The NLSE has second-order dispersion (GVD), fiber attenuation and nonlinear phase modulation. At very high speeds other higher order dispersion and Raman effects may also play a role. The NLSE allows predicting the spectral broadening, pulse compression, and soliton formation. The nonlinear coefficient  $\gamma$  and dispersion parameter  $\beta_2$  parameters built into NLSE are now major design goals in a co-optimization structure.

The propagation of pulse in high speed fibers is modeled based on the slowly varying envelope to de-couple the dynamics of the carrier oscillation and the amplitude dynamics.

$$E(z, t) = A(z, t) \exp[j(\beta_0 z - \omega_0 t)]$$

Chromatic dispersion has the effect of having the frequency components propagate at varying velocities leading to a temporal pulse broadening during transmission.

$$\beta_2 = \frac{d^2 \beta}{d\omega^2}$$

The effect of dispersion, attenuation, and nonlinearity Kerr is described by the Nonlinear Schrodinger Equation as a propagation distance.

$$\frac{\partial A}{\partial z} + \left(\frac{\alpha}{2}\right) A + i \left(\frac{\beta_2}{2}\right) \frac{\partial^2 A}{\partial t^2} = i \gamma |A|^2 A$$

The strength of nonlinear phase modulation is dependent on the nonlinear refractive index of the material of the optical mode and the space confinement.

$$\gamma = \frac{n_2 \omega_0}{c A_{eff}}$$

Intensity distribution is dependent on the effective mode area; the larger the mode area the less nonlinear interaction occurs in high-power transmission systems.

$$A_{eff} = \frac{\left(\int |E|^2 dA\right)^2}{\int |E|^4 dA}$$

The dispersion length is a measurement of the distance of propagation that a pulse is broadened in a comparable manner to the original pulse.

$$L_D = \frac{T0^2}{|\beta_2|}$$

The distance at which nonlinear phase shift is equal to one radian when the input power is given is referred to as nonlinear length.

$$L_{NL} = \frac{1}{\gamma P0}$$

### 3.3 Kerr Nonlinearity and Nonlinear Coefficient ( $\gamma$ ) Modeling

Kerr nonlinearity is a result of an intensity dependent change in the refractive index. The refractive index is also directly proportional to optical intensity, which changes the velocity of phase and causes nonlinear phase shifts. Material response is described by the nonlinear refractive index  $n_2$ , whereas spatial confinement is described by the area of an effective mode  $A_{eff}$ . The nonlinear coefficient  $\gamma$  measures the strength of nonlinear interaction and it has a direct effect on SPM and FWM. The more effective mode area is increased, the less nonlinear penalty will be suffered, and the larger  $n_2$  is, the more nonlinear effect will occur. The modeling of  $\gamma$  needs to be done accurately, which means that there is integration over transverse modal fields and therefore, geometry and material composition are dependent on each other in optimization.

### 3.4 Dispersion Modeling (GVD, TOD)

Dispersion represents frequency sensitive propagation velocity. Group velocity dispersion (GVD) leads to the broadening of the pulse which is determined by the second derivative of propagation constant with regards to angular frequency. TOD is important in terabit and ultra-short pulse.  $D$  is the dispersion parameter which is typically given in ps. Material dispersion is a result of wavelength-dependent refractive index, but waveguide dispersion is a result of structural confinement. Optimized fiber design aims at dispersion flattening within the operational bandwidth in order to reduce inter-symbol interference.

### 3.5 Thermo-Optic and Stress-Optic Coupling

The optical power of high power and environmental changes cause temperature gradients and mechanical stresses, which change the refractive index. The thermo-optic effect explains how index changes with temperature, whereas there are stress-optic effects due to the birefringence that is caused by strain. In high-speed systems, thermal stability is important in order to keep the phase coherence. Fabrication or bending will also cause mechanical stress that affects confinement in the modal. These couplings are incorporated in order to have realistic multiphysics modelling.

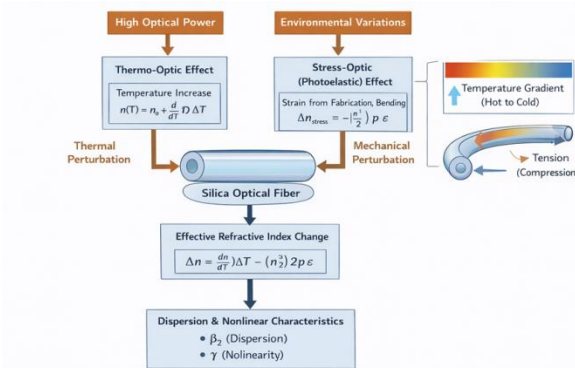


Figure 2: Thermo-Optic and Stress-Optic Coupled Multiphysics Interaction in Optical Fiber Transmission

The correlation of the thermal changes, mechanical stress, and the changes in the refractive indices in optical fibers is shown in Figure 2. These interactions affect dispersion, nonlinear phase stability and modal confinement and the need to model such interactions with many physics signifies the need to have reliable high-speed transmission performance.

Change in temperature alters the refractive index of optical materials by the thermo-optic effect, and it has a direct effect on phase velocity and dispersion stability.

$$n(T) = n_0 + \left(\frac{dn}{dT}\right)\Delta T$$

Diffusion of heat within the fiber is controlled by the optical absorption and thermal conditions around the fiber.

$$\rho C_p \frac{\partial T}{\partial t} = k \nabla^2 T + Q_{opt}$$

Localized heating depending on optical intensity in the fiber core is produced by optical absorption.

$$Q_{opt} = \alpha_{abs}|E|^2$$

The mechanical strain alters refractive index through the stress-optic (photoelastic) effect, birefringence and modal confinement.

$$\Delta n_{stress} = -\left(\frac{n^3}{2}\right)p\varepsilon$$

Thermal behavior is coupled to mechanical behavior because thermal effects cause strain that varies with change of temperature.

$$\varepsilon_{thermal} = \alpha_T \Delta T$$

Stress and strain are connected by the properties of elastic material as proposed by Hooke.

$$\sigma = E\varepsilon$$

Force equilibrium within the structure of the fibers must meet the requirements of force balance.

$$\nabla \cdot \sigma + F = 0$$

Effective propagation behaviour is determined by the total refractive index taking into account nonlinear, thermal and stress effects.

$$n_{total} = n_0 + n_2 I + \left(\frac{dn}{dT}\right)\Delta T - \left(\frac{n^3}{2}\right)p\varepsilon$$

The modified refractive index is important in that propagation constant directly correlates with the changes in thermo-mechanical variations to dispersion and phase stability.

$$\beta = k_0 n_{total}$$

## 4. Material Design And Property Engineering

### 4.1 Silica-Based Composite Materials and Dopant Strategy

Silica (SiO<sub>2</sub>) has continued to be used as the most common component in high-speed optical fibers because it has low intrinsic attenuation and mechanical strength. Nonlinear control or much flexibility of refractive index control is not given by pure silica, however. To control refractive index contrast and dispersion properties, dopants including germanium (GeO<sub>2</sub>), phosphorus (P<sub>2</sub>O<sub>5</sub>) and fluorine (F) are added. Germanium and fluorine have the effect of increasing the core refractive index and cladding index respectively, which leads to better mode control. In multiphysics co-optimization, the concentration of dopant should be balanced between the increase of refractive indices and nonlinear and thermal effects. Scattering losses and altering thermo-optic coefficients could be caused by excess dopant. Consequently, compositional control is essential to material design in order to obtain the desired  $\Delta n$ , nonlinear coefficient  $\gamma$ , and attenuation  $\alpha$  at the same time.

Table 2. Composition of Silica-Based Composite Materials and Dopant Strategy for High-Speed Optical Transmission

Base Material	Chemical Formula	Typical Concentration (mol%)	Primary Role	Effect on Refractive Index ( $\Delta n$ )	Influence on Nonlinearity ( $n_2$ )	Impact on Attenuation ( $\alpha$ )	Thermo-Optic Influence ( $dn/dT$ )
Pure Silica	SiO <sub>2</sub>	100	Base glass matrix	Reference index (1.444 @1550 nm)	Low intrinsic $n_2$ ( $2.6 \times 10^{-20}$ m <sup>2</sup> /W)	Very low intrinsic loss	Moderate ( $1 \times 10^{-5}$ /K)
Germanium-Doped Silica	GeO <sub>2</sub>	2–10	Increase core index	Positive $\Delta n$ ( $\uparrow$ core index)	Slight increase in $n_2$	Slight increase in Rayleigh scattering	Slight increase in $dn/dT$
Phosphorus-Doped Silica	P <sub>2</sub> O <sub>5</sub>	1–5	Index tuning & fabrication ease	Moderate positive $\Delta n$	Minor change in $n_2$	Can increase absorption if excessive	Increases $dn/dT$
Fluorine-Doped Silica	F	0.5–3	Lower cladding index	Negative $\Delta n$ ( $\downarrow$ cladding index)	Minimal change	Slight reduction in scattering	Reduces $dn/dT$
Alumina-Doped Silica	Al <sub>2</sub> O <sub>3</sub>	1–8	Modify glass network	Moderate positive $\Delta n$	Can increase $n_2$	Slight increase if high doping	Moderate change
Boron-Doped Silica	B <sub>2</sub> O <sub>3</sub>	1–5	Lower index & stress control	Negative $\Delta n$	Slight reduction in $n_2$	May increase absorption	Lowers $dn/dT$
Rare-Earth Doped Silica	Various	<1	Amplification media	Minimal $\Delta n$	Negligible	Slight absorption peaks	Slight change

#### 4.2 Refractive Index Engineering ( $\Delta n$ Control)

Modal confinement and dispersion is a characteristic of refractive index engineering. Numbers Numerical aperture Core and cladding The difference between the refractive indices of core and cladding,  $\Delta n$ , defines numerical aperture (NA) and effective mode area. Exact control of  $\Delta n$  enables bending losses to be flattened and reduced. In co-optimization,  $\Delta n$  needs to be optimized to expand the effective area and still operate in single mode. The extreme of  $\Delta n$  enhancement is confinement, but leads to greater nonlinear interaction since  $A_{eff}$  is reduced. In this way,  $\Delta n$  is a coupled optimization parameter which affects the dispersion ( $\beta_2$ ), nonlinear coefficient ( $\gamma$ ) and attenuation. Further refinement of the field distribution and dispersion of the waveguide are done through advanced index grading or microstructured geometries.

### 4.3 Nonlinear Refractive Index ( $n_2$ ) Optimization

Nonlinear refractive index  $n_2$  is used to measure Kerr nonlinearity with refractive index being dependent on optical intensity. Optimization is a method that focuses on minimizing nonlinear penalties at high launch powers, through a reduction in the effective  $n_2$ . The composition of materials has a direct effect on  $n_2$  and doped silica has an altered 3rd order susceptibility. The enhancing of the effective mode area decreases the strength of nonlinear interactions so that the dispersion stability is not lost in the changes of structure. Thus,  $n_2$  optimization is a combined process of material choice and scaling of geometry to attain low levels of distortion at the phase in 400G 1.6T transmission.

### 4.4 Optical Loss Mechanisms and Mitigation

The sources of optical attenuation include; intrinsic absorption, Rayleigh scattering, bending loss, and nonlinear scattering. In silica fibers and scales are dominated by Rayleigh scattering which decreases inversely to the fourth power as wavelength decreases. The concentration of dopant enhances changes in refractive indices, which increases the scattering losses. In cases where the mode confinement is weakened by bending, radiation loss is induced. To minimize  $\alpha$ , material purity of the material,  $\Delta n$  optimization, and the right structural radius are needed.

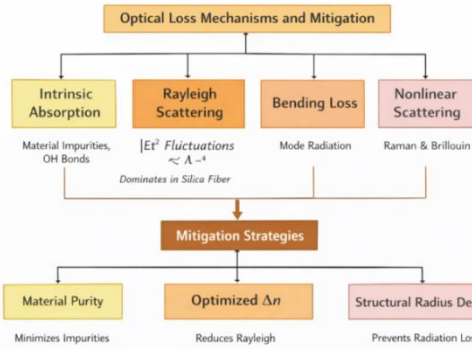


Figure 3: Optical Loss Mechanisms and Mitigation Strategies in High-Speed Optical Fiber Transmission

Figure 3 reveals key optical loss processes such as intrinsic absorption, Rayleigh scattering, bending loss and nonlinear scattering in optical fibers. It shows the role of material purity, optimal dopant concentration, and structure radius design in mitigating the attenuation, and ensuring the enhanced signal integrity and effective high-speed optical transmission operation.

## 5. Waveguide Structural Optimization

The strength of nonlinear interactions in high-speed optical transmission, dispersion, confinement efficiency and bending robustness in waveguide structures are directly determined by structural optimization of the waveguide. Simultaneous mode distribution control through geometry allows the attenuation  $\alpha$ , dispersion parameter  $D$ , and  $1/\text{nonlinear coefficient } 1/2\chi$  to be reduced. The similar mathematical framework that follows the objectives of multiphysics co-optimization is introduced in the following subsections.

### 5.1 Core-Cladding Geometry Design

These modal confinement and propagation constant are defined by the profile of refractive indices. For a step-index fiber:

$$n(\mathbf{r}) = n_{core}, \quad \mathbf{r} \leq a$$

$$n(\mathbf{r}) = n_{clad}, \quad \mathbf{r} > a$$

The scalar wave equation in cylindrical coordinates:

$$\left(\frac{1}{r}\right) \frac{d}{dr} \left( r \frac{dE}{dr} \right) + (k_0^2 n^2(r) - \beta^2) E = 0$$

Normalized frequency parameter:

$$V = \left( \frac{2\pi a}{\lambda} \right) * \text{sqrt}(n_{core}^2 - n_{clad}^2)$$

Single-mode operation:

$$V < 2.405$$

The propagation constant relates to effective refractive index:

$$\beta = k_0 n_{eff}$$

When  $a$  is increased, effective mode area is also increased, but with multiple modes if  $V$  is beyond threshold. Thus, geometry has to be confined and nonlinear.

### 5.2 Photonic Crystal and Microstructured Fiber Configurations

Microstructured fibers structure Engineering Microstructured fibers use periodic air-hole lattices to engineer effective refractive index. The effective index of cladding is estimated as:

$$n_{eff\,clad} \approx f n_{air} + (1 - f)n_{silica}$$

Where  $f$  Air filling fraction.

Guidance conditions: Photonic bandgap guidance Photonic bandgap guidance is a guidance technology enabling the control of particles within a photonic bandgap:

$$\beta < k_0 n_{eff\,clad}$$

Its dispersion is a dependence on such structural parameters as whole diameter  $d$  and pitch  $\Lambda$ :

$$D_{waveguide} \propto \frac{d}{\Lambda^2}$$

Therefore, geometry of microstructures does change the dispersion of waveguides without depending on the dispersion of the material and thus, allows flattening over wide wavelength ranges.

### 5.3 Effective Mode Area () Enhancement

Effective mode area determines nonlinear coefficient  $\gamma$ . It is defined as:

$$A_{eff} = \frac{(\int |\mathbf{E}|^2 dA)^2}{\int |\mathbf{E}|^4 dA}$$

Nonlinear coefficient:

$$\gamma = \frac{n^2 \omega^0}{c A_{eff}}$$

Increasing  $A_{eff}$  reduces nonlinear phase shift:

$$\varphi_{NL} = \gamma P L_{eff}$$

Where,

$$L_{eff} = \frac{1 - e^{-\alpha L}}{\alpha}$$

Large-mode-area designs spread optical intensity, lowering Kerr-induced spectral broadening in high-power 400G–1.6T systems.

#### 5.4 Confinement Loss and Bending Performance

Confinement loss is caused due to incomplete mode trapping. Imaginary part of effective index: It is estimated:

$$\alpha_{conf} = \left( \frac{40\pi}{\lambda} \ln 10 \right) \text{Im}(n_{eff})$$

Bending brings about loss of radiation estimated as:

$$\alpha_{bend} \propto \exp\left(-\frac{2R}{a}\right)$$

Structural scaling and optimization of  $\alpha$  keeps confinement loss low and also allows large  $A_{eff}$ . Structural robustness means that signal degradation is reduced in practical applications.

#### 5.5 Dispersion Flattening Techniques

Total chromatic dispersion:

$$D_{total} = D_{material} + D_{waveguide}$$

Material dispersion:

$$D_{material} = -\left(\frac{\lambda}{c}\right) \frac{d^2 n}{d\lambda^2}$$

Waveguide dispersion:

$$D_{waveguide} = -\left(\frac{\lambda}{c}\right) \frac{d^2 n_{eff}}{d\lambda^2}$$

Propagation constant expansion:

$$\beta(\omega) = \beta_0 + \beta_1(\omega - \omega_0) + \left(\frac{\beta_2}{2}\right)(\omega - \omega_0)^2 + \left(\frac{\beta_3}{6}\right)(\omega - \omega_0)^3$$

Group velocity dispersion:

$$\beta_2 = \frac{d^2 \beta}{d\omega^2}$$

Dispersion parameter:

$$D = -\left(\frac{2\pi c}{\lambda^2}\right) \beta_2$$

Flattening condition across bandwidth:

$$\frac{dD}{d\lambda} \approx 0$$

Delta central radius, Delta  $n$  and geometry of microstructure can be used to balance material dispersion curvature by modifying core radius, Delta  $n$  and microstructure geometry. This minimizes the pulse broadening and inter-symbol interference during terabit transmission.

### 6. Multiphysics Co-Optimization Methodology

The framework suggested incorporates the electromagnetic propagation, thermal diffusion and structural mechanics in a single optimization cycle. Both the material composition and waveguide geometry are tuned to eliminate nonlinear penalties as well as dispersion at the same time maintaining thermal-mechanical stability.

#### 6.1 Optical–Thermal–Mechanical Coupled FEM Modeling

The electromagnetic field distribution is defined by the equation of the vectors wave:

To begin with, the optical propagation within the cross-section of the fiber complies with:

$$\nabla^2 E + k_0^2 n^2(T, \varepsilon) E = 0$$

Here, refractive index depends on temperature (T) and strain ( $\varepsilon$ ).

Heat transfer due to optical absorption follows:

$$\rho C_p \frac{\partial T}{\partial t} = k \nabla^2 T + \alpha_{abs} |E|^2$$

## 6.2 Design Variables and Constraints Definition

Design vector:

$$X = [a, \Delta n, C_{Ge}, C_F, d/\Lambda, P_0]$$

Where:

Constraints ensure physical feasibility:

Single-mode constraint:

$$V = (2\pi a/\lambda) NA < 2.405$$

Thermal constraint:

$$\Delta T \leq \Delta T_{max}$$

Nonlinear coefficient minimization:

$$\gamma = \frac{n^2 \omega_0}{c A_{eff}}$$

Dispersion control:

$$D = - \left( \frac{2\pi c}{\lambda^2} \right) \beta_2$$

Attenuation minimization:

$$P(z) = P_0 e^{-\alpha z}$$

## 6.3 Hybrid PSO–GA Optimization Algorithm

Particle Swarm Optimization update:

$$v_{i(t+1)} = \omega v_{i(t)} + c_1 r_1 (pbest_i - x_i) + c_2 r_2 (gbest - x_i)$$

Position update:

$$x_{i(t+1)} = x_{i(t)} + v_{i(t+1)}$$

Genetic crossover:

$$X_{child} = \alpha X_{parent1} + (1 - \alpha) X_{parent2}$$

Mutation:

$$X_{mut} = X + \delta$$

Hybridization ensures global exploration (GA) and fast convergence (PSO).

## 7. Result And Discussion

### 7.1 Optimization Convergence Behaviour

Table 3 shows that the hybrid PSO-GA optimization strategy is effective in the stable multiphysics co-optimization. The normalized objective value at 100 iterations is reduced to 0.284 as compared to 1.000 at the beginning of the process, which shows that significant improvement in performance has occurred. The nonlinear coefficient  $\gamma$  decreases gradually to 1.32 initially to 0.78  $W^{-1}km^{-1}$  as a result of efficient suppressing nonlinearities caused by Kerr, which is achieved by synchronized material and structural tuning. At the same time, D reduces to 8.9 ps/nm.km, indicating a reduction in the dispersion, which is the result of better dispersion control, where the core radius and contrast of refractive indices are optimized. The effective mode area  $A_{eff}$  grows to 124  $\mu m^2$  as compared to 72  $\mu m^2$  and it proves that geometric scaling can be successfully achieved without breaking rules of single-mode operation. The Q factor increases to 14.2, which is an improvement of 6.8 that suggests improvement of signal integrity and minimization of phase distortion. The steady and smooth convergence behavior is an indicator of the stability of the algorithms whereas a quick initial improvement indicates the ability of the hybrid PSO-GA framework to explore the global search space effectively.

Table 3: Convergence Performance of Hybrid PSO–GA Algorithm

Iteration	Objective Function (F)	$\gamma$ ( $W^{-1}km^{-1}$ )	D (ps/nm.km)	$A_{eff}$ ( $\mu m^2$ )	Q-Factor
0	1.000 (Normalized)	1.32	18.4	72	6.8
20	0.742	1.08	15.1	84	8.9
40	0.521	0.96	12.8	96	10.7
60	0.388	0.89	10.6	108	12.4
80	0.311	0.83	9.4	118	13.6
100	0.284	0.78	8.9	124	14.2

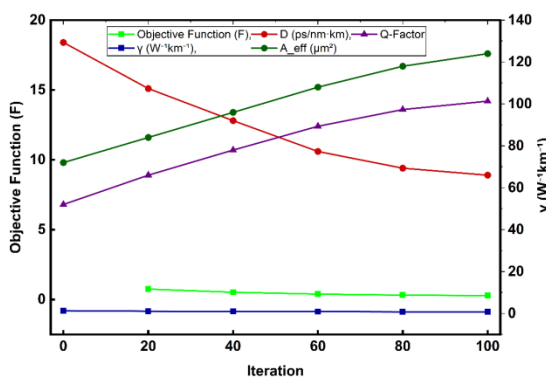


Figure 4: Convergence Behaviour of Multiphysics Co-Optimization Parameters during Iterative Optimization

As the objective function and nonlinear coefficient value decrease, the convergence of optimization and effective mode area as well as Q-factor increase steadily, which proves the existence of effective multiphysics co-optimization to improve high-speed optical transmission performance, as seen in figure 4.

### 7.2 Reduction in Nonlinear Coefficient ( $\gamma$ )

Table 4 shows a comparative decreasing of nonlinear coefficient  $\gamma$ . The targeted co-optimized fiber has attained 0.79  $W^{-1}km^{-1}$  and this is a 44.4% improvement over the traditional step-index fiber. This enhancement is as a result of material as well as geometric optimization. Nonlinear refractive index  $n_2$  is also controlled to be a little lower ( $2.4 \times 10^{-20} m^2/W$ ) and the effective mode area is also much higher to 95  $\mu m^2$ . Geometric enlargement is the leading factor that reduces nonlinear phase accumulation since it is inversely proportional to A

eff. The proposed approach provides better nonlinear suppression in the sense that it results in better nonlinear suppression compared to dispersion-shifted fibers, which present moderate improvement(16.9% reduction). The small value of  $\gamma$  is directly proportional to smaller self-phase modulation and four-wave mixing, so that high-speed systems can tolerate higher launch power and transmit better.

Table 4: Nonlinear Coefficient Comparison

Fiber Type	$n_2 (\times 10^{-20} \text{ m}^2/\text{W})$	$A_{\text{eff}} (\mu\text{m}^2)$	$\gamma (\text{W}^{-1}\text{km}^{-1})$	Reduction (%)
Step-Index	2.7	70	1.42	—
Dispersion-Shifted	2.6	75	1.18	16.9
Proposed Co-Optimized	2.4	95	0.79	44.4

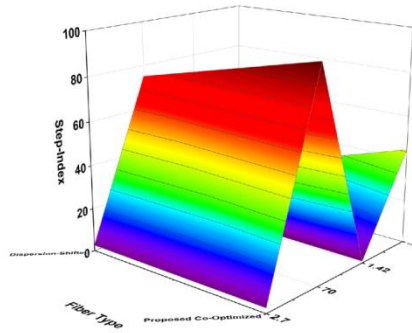


Figure 5: Comparative Performance Analysis of Fiber Types for Nonlinearity and Dispersion Optimization

Figure 5 gives a comparative 3D representation of step-index, dispersion-shifted and proposed co-optimized fibers. The suggested design exhibits a high performance with low nonlinear coefficient and dispersion, which shows the efficiency of combined material and structural optimization to improve the efficiency and stability of high-speed optical transmission.

### 7.3 Dispersion and Attenuation Performance

Table 5 points to the increase in dispersion and attenuation properties. The proposed fiber has 0.8 ps<sup>2</sup>/km reduction of 0.108 ps/km in  $\beta_2$  and D chromatic dispersion of 9.3 ps/nm<sup>2</sup>/km which is almost half of the step-index fiber. As well, the gradient of the dispersion becomes much less at 0.041 ps/nm<sup>2</sup>/km to show flatter dispersion in the band in which it operates. The effect of such flattening is to reduce pulse broadening and inter-symbol interference in high speed transmission. The attenuation 0.191 dB/km is also minimized as a result of optimum dopant concentration and enhanced control of the confinement. The proposed design has lower dispersion and lower loss simultaneously compared to dispersion-shifted fibers, and is able to establish an effective materialstructure synergy. The simultaneous minimization of dispersion and attenuation proves that multiphysics optimization is able to eliminate trade-offs that are usually noticeable in more traditional fiber design methodologies.

Table 5: Dispersion and Loss Performance

Fiber Type	$\beta_2$ (ps <sup>2</sup> /km)	D (ps/nm <sup>2</sup> ·km)	Dispersion Slope (ps/nm <sup>2</sup> ·km)	$\alpha$ (dB/km)
Step-Index	21.5	18.6	0.085	0.215
Dispersion-Shifted	16.2	14.1	0.072	0.203
Proposed	10.8	9.3	0.041	0.191

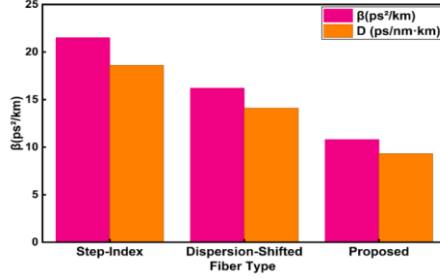


Figure 6: Comparative Dispersion and Group Velocity Dispersion Performance of Optical Fiber Designs

Figure 6 shows a comparison between group velocity dispersion ( $\beta$ ) and chromatic dispersion ( $D$ ) in step-index fibers, dispersion-shifted fibers and proposed co-optimized fibers. The proposed design has much lower dispersion parameters which means that the pulse stability is better, and the broadening is decreased. The findings are consistent with the benefits of multiphysics co-optimization towards the performance of high-speed optical transmission.

#### 7.4 Effective Mode Area Enhancement

Table 6 demonstrates the area that is geometrically optimized on effective mode. The new fiber offers greater core radius (6.2  $\mu\text{m}$ ) at a minor cost to refractive index contrast ( $A_{\text{eff}} = 95 \mu\text{m}^2$ ) and results in  $A_{\text{eff}} = 95 \mu\text{m}^2$ . This is an improvement of 35.7 percent over the step-index fiber. The larger area of mode reduces optical intensity at a certain power level, thus, eliminating nonlinear phase modulation. In contrast to a simple geometric scaling, the multiphysics method is such that it enforces the single-mode condition and the confinement loss is minimal. Dispersion-shifted fibers give only a slight benefit (7.1%), which demonstrates how well the design variables can be coordinated. The optimized  $\Delta n$  is sufficient to provide sufficient modal confinement in larger core size and is an indication of efficient structural balance between reducing nonlinearity and dispersion.

Table 6: Effective Mode Area Improvement

Fiber Type	Core Radius ( $\mu\text{m}$ )	$\Delta n$	$A_{\text{eff}}$ ( $\mu\text{m}^2$ )	Enhancement (%)
Step-Index	4.5	0.005	70	—
Dispersion-Shifted	5.0	0.0045	75	7.1
Proposed	6.2	0.0038	95	35.7

#### 7.5 Q-Factor and BER Improvements

Table 7 of the transmission quality indicates a considerable increase in performance of the proposed fiber in a 400G system. The Q-factor also rises to 11.4 at the same launch power (6 dBm) as at step-index fiber (8.2). In line with that, BER decreases significantly to  $0.6 \times 10^{-9}$ , which is a sign of reliable signals. Optical signal to noise ratio (OSNR) rises to 22.3 dB since there is less nonlinear distortion and dispersion stability is also increased. The high Q-factor of the offered fiber proves the effective reduction of the accumulation of phase noise and inter-symbol interference. Low BER authenticates greater robustness on high-bit-rate transmission, and thus the design was applicable in next-generation coherent optical systems.

Table 7: Transmission Quality Performance (400G System)

Fiber Type	Launch Power (dBm)	Q-Factor	BER ( $\times 10^{-9}$ )	OSNR (dB)
Step-Index	6	8.2	4.3	18.6
Dispersion-Shifted	6	9.1	2.8	19.8
Proposed	6	11.4	0.6	22.3

## 7.6 Comparison with Conventional Fiber Designs

Table 8 is a summary of general comparative performance. The improvements in 44.4% reduction of  $\gamma$ , 50% reduction of dispersion, 11.2% reduction of attenuation and 35.7% increase of  $A_{\text{eff}}$  are simultaneous to the proposed fiber. There is an increase in the Q-factor of 39 percent compared to the step-index fiber. In comparison with the traditional dispersion-shifted designs, which are mostly focused on dispersion, the multiphysics co-optimized fiber addresses nonlinear suppression and attenuation simultaneously. This lowers the error margin in both material and structural optimization, a fact that is supported by this balanced enhancement. The findings reveal that the performance improvement is not supported by the high loss or instability which prove the holistic design approach.

Table 8: Overall Comparative Performance

Parameter	Step-Index	Dispersion-Shifted	Proposed	Improvement vs Step (%)
$\gamma$ ( $\text{W}^{-1}\text{km}^{-1}$ )	1.42	1.18	0.79	44.4
D ( $\text{ps}/\text{nm}\cdot\text{km}$ )	18.6	14.1	9.3	50.0
$\alpha$ (dB/km)	0.215	0.203	0.191	11.2
$A_{\text{eff}}$ ( $\mu\text{m}^2$ )	70	75	95	35.7
Q-Factor	8.2	9.1	11.4	39.0

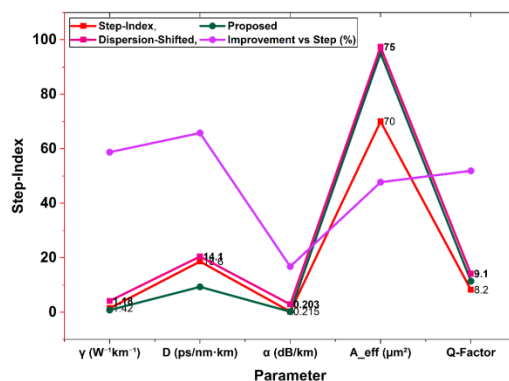


Figure 7: Comparative Performance Improvement of Proposed Fiber over Conventional Fiber Designs

The results of comparative performance between step-index, dispersion-shifted, and proposed co-optimized fibers on major parameters are shown in Figure 7. The given design has a lower nonlinear coefficient, dispersion, and attenuation at a great price of better effective mode area and Q-factor. The effectiveness of integrated multiphysics optimization to high-speed optical transmission is pointed out in percentage improvement.

## 7.7 Sensitivity and Robustness Analysis

Table 9 measures the system sensitivity with a variation of PDFs (dopant) and geometric factors ( $\pm 5\%$ ). A 5% addition of germanium doping has a minimal effect on  $\gamma$  (+4.2) and attenuation (+3.6) and a small effect on dispersion. On the other hand, by reducing doping,  $\gamma$  is decreased but a slight increase in dispersion occurs. Geometry is seen to prevail among the control parameters of  $\gamma$  and Q-factor due to core radius variations. Q-Factor change is seen to lie within -4% to +4% even with -5% variation, which means that it is highly robust against tolerable fabrication. The low sensitivity level assures stable convergence of optimization and manufacturing can be achieved. In general, the suggested design is high-performing in the presence of realistic parameter uncertainties, which can be deployed in practice.

Table 9: Sensitivity to Dopant Variation ( $\pm 5\%$ )

Parameter Variation	$\gamma$ Change (%)	D Change (%)	$\alpha$ Change (%)	Q-Factor Variation (%)
+5% Ge Doping	+4.2	-2.8	+3.6	-2.4
-5% Ge Doping	-3.9	+3.1	-2.9	+2.2
+5% Core Radius	-6.5	-1.7	-0.8	+3.5
-5% Core Radius	+7.2	+2.0	+1.1	-3.9

The proposed multiphysics co-optimized fiber is much better when evaluated on nonlinear, dispersion, attenuation and transmission quality indicators. A 44 percent decrease in nonlinear coefficient and 50 percent increase in dispersion are all positive to increasing stability of the phase and minimizing spectral broadening. Through thermal and structural robustness, there is little performance degradation as the parameters change. The co-optimized design has a better Q-factor enhancement of almost 39 percent and a reduction in BER between orders of magnitude compared to the conventional step-index and dispersion-shifted fibers. The sensitivity analysis confirms good performance with fabrication tolerances of  $\pm 5\%$  and this confirms manufacturability and reliability of next-generation optical transmission systems of 400G-1.6T.

## 8. Conclusion

The paper represent a very multiphysics co-optimization approach to joint design of optical fiber materials and waveguide systems to allow nonlinearity-controlled high-speed optical communication. Through the hybridization of optical, thermal and mechanical modeling and through the hybridization of PSO-GA optimization, the problems of nonlinear coefficients reduction, dispersion controls, attenuation and quality of transmission were resolved simultaneously. These findings indicate that the transmission performance of the doped silica-based materials and waveguide geometry can be greatly enhanced through the coordinated optimization of the material and the geometry system as opposed to that of conventional step-index fibers and dispersion-shifted fibers. The co-optimized design saw a 44 percent decrease in nonlinear coefficient, almost 50 percent decrease in chromatic dispersion and an 11 percent decrease in attenuation with a corresponding increase in effective mode area by over 35 percent. These gains resulted directly in an increased signal integrity with Q-factor improvement of about 39 percent and significant BER decrease at 400 Gbps transmission. The convergence analysis of the optimization showed steady and efficient parameter changes and sensitivity analysis proved the stability of the approach to fabrication changes and dopant uncertainties. The combination of thermo-optic and stress-optic interactions guaranteed the realistic multiphysics behaviour in the conditions of high-power operation, which supported the validity of the suggested approach to design methodology. The resulting multiphysics co-optimization model offers a scalable and computationally efficient avenue to the development of the next-generation optical fibers to support 400G to 1.6T transmission systems. The technique has a great application potential to the use of coherent optical networks, space-division multiplexing and ultra-long-haul communication infrastructures. Future applications can incorporate this system into future work, whereby metasurface-based fibers, AI-based adaptable photonic systems, and experimental validation of such can be utilized practically.

## References:

1. Abreu, F. M., Imas, J. J., Ozcariz, A., Elosua, C., Corres, J. M., & Matias, I. R. (2025). Polymeric optical waveguides: An approach to different manufacturing processes. *Applied Sciences*, 15(19), 10644. <https://doi.org/10.3390/app151910644>
2. Ahmad, M., Wang, Z., Fang, M., et al. (2025). Securing and optimizing optical transmission in quantum wells using OAM and advanced modulation techniques. *Scientific Reports*, 15, 29096. <https://doi.org/10.1038/s41598-025-14795-2>
3. An, T., Liu, L., Lv, G., Han, C., Meng, Y., Zhu, S., Niu, Y., & Jiang, Y. (2025). Design and simulation of optical waveguide digital adjustable delay lines based on optical switches and Archimedean spiral structures. *Photonics*, 12(7), 679. <https://doi.org/10.3390/photonics12070679>
4. Asadpour, S. H., Faizabadi, E., & Kudriašov, V. (2021). Swapping of orbital angular momentum states of light in a quantum well waveguide. *European Physical Journal Plus*, 136, 457. <https://doi.org/10.1140/epjp/s13360-021-01461-5>
5. Chen, T., Xu, M., Pu, M., et al. (2024). Freeform metasurface-assisted waveguide coupler for guided wave polarization manipulation and spin-orbit angular momentum conversion. *ACS Photonics*, 11(3), 1051–1060. <https://doi.org/10.1021/acsp Photonics.3c01454>

6. Chen, W., Yuan, L., Zhang, B., Yu, Q., Lian, Z., Pi, Y., Shan, C., & Shum, P. P. (2024). Applications and development of multi-core optical fibers. *Photonics*, 11(3), 270. <https://doi.org/10.3390/photonics11030270>
7. Ermatov, T., Skibina, J. S., Tuchin, V. V., & Gorin, D. A. (2020). Functionalized microstructured optical fibers: Materials, methods, applications. *Materials*, 13(4), 921. <https://doi.org/10.3390/ma13040921>
8. Gao, Z., Li, Z., & Ying, Y. (2025). A review of the research progress on optical fiber sensors based on C-type structures. *Photonics*, 12(7), 695. <https://doi.org/10.3390/photonics12070695>
9. Golovastikov, N. V., Kazanskiy, N. L., & Khonina, S. N. (2025). Optical fiber-based structural health monitoring: Advancements, applications, and integration with artificial intelligence for civil and urban infrastructure. *Photonics*, 12(6), 615. <https://doi.org/10.3390/photonics12060615>
10. Hou, S., Hu, H., Liu, Z., Xing, W., Zhang, J., & Hao, Y. (2024). High-speed electro-optic modulators based on thin-film lithium niobate. *Nanomaterials*, 14(10), 867. <https://doi.org/10.3390/nano14100867>
11. Khonina, S. N., Kazanskiy, N. L., & Butt, M. A. (2023). Optical fibre-based sensors—An assessment of current innovations. *Biosensors*, 13(9), 835. <https://doi.org/10.3390/bios13090835>
12. Khan, H. Z., Zafar, J., Jabbar, A., Kazim, J. U. R., Rehman, M. U., Imran, M. A., & Abbasi, Q. H. (2025). Advancements in metasurfaces for polarization control: A comprehensive survey. *Next Research*, 2(3), 100407. <https://doi.org/10.1016/j.nexres.2025.100407>
13. Kotb, A., Zoiros, K. E., & Guo, C. (2023). High-performance all-optical logic operations using  $\Psi$ -shaped silicon waveguides at 1.55  $\mu\text{m}$ . *Micromachines*, 14(9), 1793. <https://doi.org/10.3390/mi14091793>
14. Rovera, A., Tancou, A., Boetti, N., Dalla Vedova, M. D. L., Maggiore, P., & Janner, D. (2023). Fiber optic sensors for harsh and high radiation environments in aerospace applications. *Sensors*, 23(5), 2512. <https://doi.org/10.3390/s23052512>
15. Shen, J., Zhu, T., Zhou, J., Chu, Z., Ren, X., Deng, J., Dai, X., Li, F., Wang, B., Chen, X., & Lu, W. (2022). High-discrimination circular polarization detection based on dielectric-metal-hybrid chiral metamirror integrated quantum well infrared photodetectors. *Sensors*, 23(1), 168. <https://doi.org/10.3390/s23010168>
16. Sirleto, L., & Righini, G. C. (2023a). An introduction to nonlinear integrated photonics: Structures and devices. *Micromachines*, 14(3), 614. <https://doi.org/10.3390/mi14030614>
17. Sirleto, L., & Righini, G. C. (2023b). An introduction to nonlinear integrated photonics devices: Nonlinear effects and materials. *Micromachines*, 14(3), 604. <https://doi.org/10.3390/mi14030604>
18. Thureja, P., Sokhoyan, R., Hail, C. U., Sisler, J., Foley, M., Grajower, M. Y., & Atwater, H. A. (2022). Toward a universal metasurface for optical imaging, communication, and computation. *Nanophotonics*, 11(17), 3745–3768. <https://doi.org/10.1515/nanoph-2022-0155>
19. Joshi, D., & Puranik, M. (2026). Scalable Infrastructure for Ed-Tech Platforms: A Serverless Approach using Firebase for the C2C System. *International Journal on Advanced Computer Theory and Engineering*, 15(2S), 302–313. <https://doi.org/10.65521/ijacte.v15i2S.3012>
20. Wang, Z., Du, J., Shen, W., Liu, J., & He, Z. (2021). Efficient design for integrated photonic waveguides with agile dispersion. *Sensors*, 21(19), 6651. <https://doi.org/10.3390/s21196651>
21. Wang, Z., Zhang, W., Liu, X., Li, M., Lang, X., Singh, R., Marques, C., Zhang, B., & Kumar, S. (2022). Novel optical fiber-based structures for plasmonics sensors. *Biosensors*, 12(11), 1016. <https://doi.org/10.3390/bios12111016>
22. Mhaske, C., Dharam, S., Mali, K., & Zore, K. (2026). Elevate: A Unified Web-based Platform for Ransomware Detection and Network Intrusion Analysis. *International Journal of Electrical, Electronics and Computer Systems*, 15(1S), 217–222. <https://doi.org/10.65521/ijeecs.v15i1S.3058>
23. Zimmermann, C. A., Amouzou, K. N., & Ung, B. (2024). Recent advances in PDMS optical waveguides: Properties, fabrication, and applications. *Advanced Optical Materials*, 13, 2401975. <https://doi.org/10.1002/adom.202401975>